

Hybrid Surfacing: Laser + MAG Electric Arc

Abstract: The article discusses technological tests involving the use of the hybrid process (laser + electric arc (MAG)) for the efficient application of layers (surfacing). The objective of the tests was to determine the effect of an additional welding power source (laser beam) on the possibility of increasing a surfacing rate (in comparison with surfacing rates obtainable using the MAG method) as well as on the formation (shaping) of the overlay weld geometry and the degree of dilution (of the base material in the overly weld). The technological tests of the hybrid (HLAW (laser + MAG)) surfacing process involved the use of steel grade 41Cr4 and filler metal grade LNM 307.

Keywords: surfacing, hybrid (laser + MAG) surfacing, steel 41Cr4, surface processing

DOI: [10.17729/ebis.2020.6/2](https://doi.org/10.17729/ebis.2020.6/2)

Introduction

Modern engineering structures and advanced technological processes increasingly often require the application of appropriate surface processing methods to provide the effective and reliable operation of structures, often exposed to ultimate stresses and very aggressive environments. Frequently, individual elements of machinery have to satisfy special requirements, particularly in relation to the core of a material and its surface. Today's surface engineering is confronted with increasingly difficult challenges which can be addressed using new and more effective technological solutions. One of such solutions providing high process efficiency is the laser radiation beam used as a heat source in surface processing methods such as hardening, surface alloying, remelting or surfacing.

The MIG/MAG arc surfacing process is commonly used in industries either as production

or repair surfacing. Increasingly often, in addition to electric arc-based method, surfacing processes involve the use of laser radiation, e.g. laser powder deposition [1, 2].

Some of the laser-based processing methods are hybrid processes. Hybrid methods are enjoying growing popularity among entrepreneurs. Although hybrid methods have been used for more than a decade now, they are still perceived as advanced and innovative welding technologies. The combination of two welding power sources results in synergy, the result of which is not a simple sum of effects of two welding power sources. Usually, the use of hybrid methods leads to increased process efficiency [3–8].

Similar to hybrid welding, hybrid surfacing involves the simultaneous use of two heat sources, i.e. laser radiation and electric arc, in the same area (Fig. 1a). Situations, where the

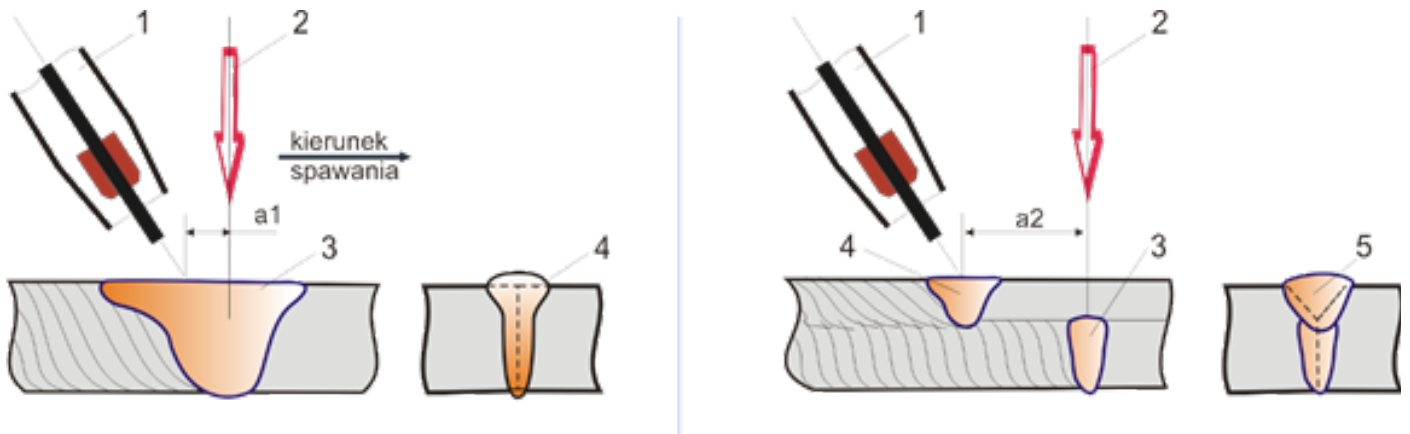


Fig. 1. Schematic diagram of the simultaneous application of the laser beam and electric arc:

- a) schematic diagram of the hybrid (laser + electric arc) welding/surfacing process (1 – arc welding torch, 2 – laser beam, 3 – liquid metal pool common for both methods, 4 – weld in cross-section);
- b) schematic diagram of the laser + electric combined method (1 – arc welding torch 2 – laser beam, 3 – liquid metal pool formed as a result of laser radiation, 4 – liquid metal pool formed as a result of electric arc effect, 5 – weld in cross-section); a_1 , a_2 – distance between the electrode wire tip and the laser beam axis

two above-named welding power sources do not interact in one liquid metal pool (Fig. 1b) are, in accordance with PN-EN ISO 15609-6:2013 [9], referred to as combined processes.

The hybrid surfacing process involving the use of laser radiation and electric arc is not very well known. The analysis of available reference publications browsed using the keyword of “hybrid surfacing” revealed that the above-named term is usually used in relation to MAG-based surfacing involving the application of induction heating. One of very few publications on the subject is a patent application concerning hybrid surfacing combining the MAG method

and the laser beam. The patent, granted on 15 June 2017 to Caterpillar Inc. (USA), is concerned with the application of laser and a surfacing process involving the use of a flux-cored wire having a specific chemical composition [10]. The patent is primarily focused on a claim related to the chemical composition of the flux-cored wire used in the surfacing process.

Advantages offered by the above-named hybrid surfacing method compared with those typical of classical surfacing processes are presented in Figure 2. The synergic interaction of two heat sources extends the range of the adjustment of surfacing process parameters affecting primary geometric parameters of overlay welds, which, in turn, directly affect both technical and economic factors decisive for surfacing process efficiency ($l_2 > l_1$ and post-surfacing processing $a_2 < a_1$) (rolling or grinding of the surface previously subjected to the surfacing process).

An additional aspect of the surfacing process is connected with the lowest possible degree of the dilution of the base material and the deposited material in the melted surfaced layer. The low coefficient of the dilution of the base material in the surfaced layer enables the obtainment of the most favourable properties (of the surfaced layer).

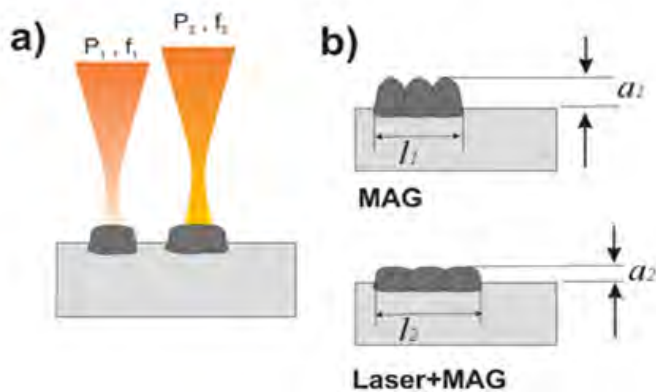


Fig. 2. HLAW method-based surfacing, a) schematic diagram presenting the determination of the laser beam focus location in relation to the surface of the material subjected to the surfacing process, b) differences between overlay weld geometries obtained using the MAG method-based surfacing and the hybrid surfacing process

Welding station

The technological welding tests of hybrid surfacing involved the use of a robotic hybrid welding station (Fig. 3) provided with a TruDisk 12002 solid-state laser having a maximum laser beam power (on the material) of 12 kW, a KUKA KR30HA industrial robot and a Phoenix 452 RC PULS MIG/MAG method EWM welding power source integrated in terms of software with the robot control system (Fig. 4). The tests also involved the use of a D70 hybrid welding head (Trumpf) provided with a collimator lens having focal length $f_{kol} = 200$ mm and a focusing lens having length $f_{og} = 400$ mm. The parameters of the arc-based process were recorded using a PCD 505 (Parameter Control and Documentation System) system, installed in the control system of the robot controller and adapted for the interaction with the hybrid head operation (Fig. 5).

The technological tests involved the use of an optical fibre having a diameter of 400 μm , enabling the obtainment of laser beam focus diameter $d_{og} = 0.8$ mm in relation to Rayleigh length $ZR = 10$ mm (for $f = 0$). The hybrid surfacing tests were performed using a defocused beam (Fig. 6a) obtained by lifting the head and the focus position upwards by 20 mm ($f = +20$ mm). In the aforesaid arrangement, the diameter of the laser beam focus was $d_{og} = 1.6$ mm (Fig. 6b). The lifting of the head by 20 mm required the lowering of the welding torch using adjustment screws so that the electrode wire tip touched the plate surface (Fig. 6c).

Test materials

The tests involved the use of 5 mm thick plates (200 mm x 100 mm) made of chromium steel 41Cr4 (1.7035) used for toughening and surface hardening. Structural steel 41Cr4



Fig. 3. Robotic hybrid welding/surfacing station with the TruDisk 12002 disc laser: a – main view, b – D70 hybrid welding/surfacing head mounted on the industrial robot wrist

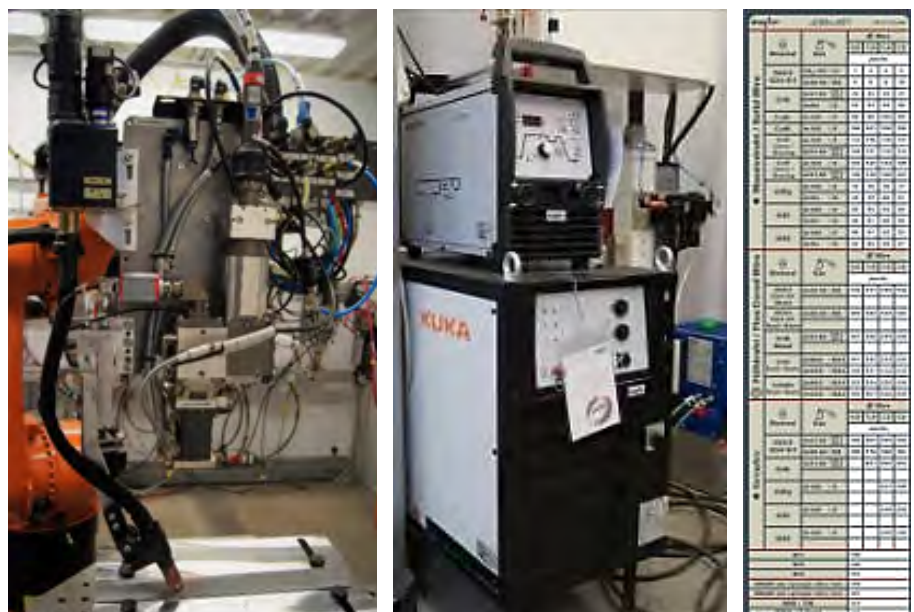


Fig. 4. Laser head for hybrid (laser + MIG/MAG) welding/surfacing (a) MIG/MAG method EWM welding power source and (b) list of machine operation programmes in the synergic mode (c)

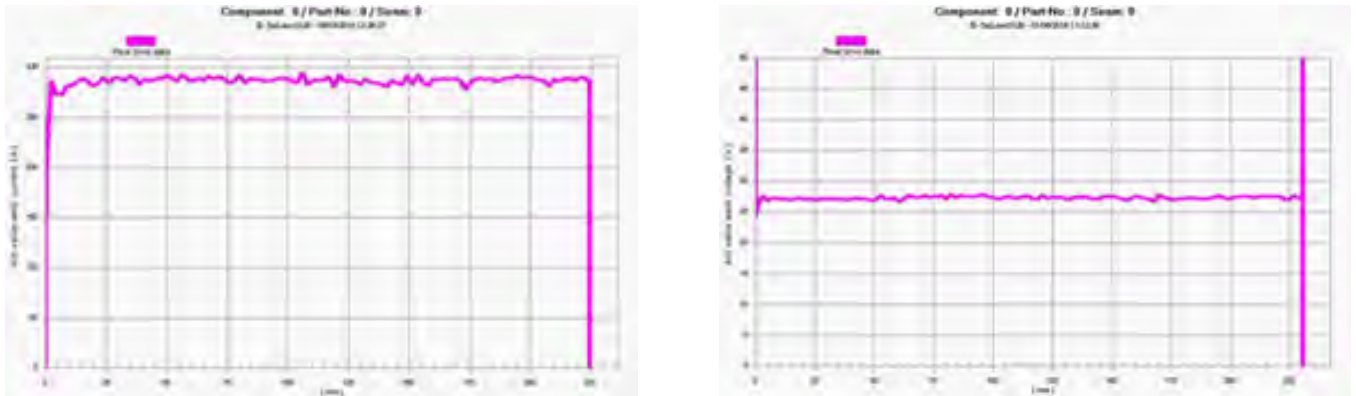
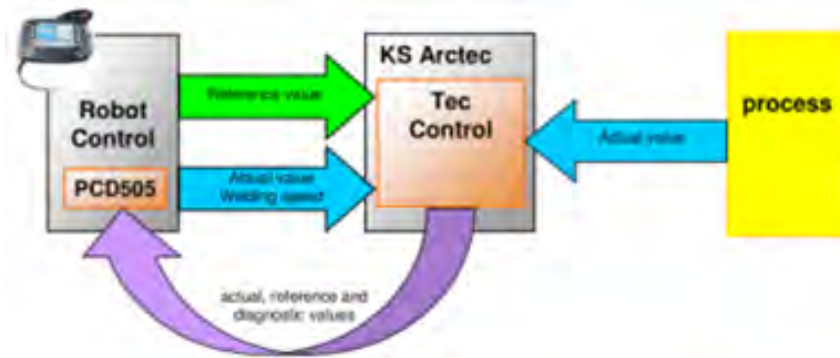
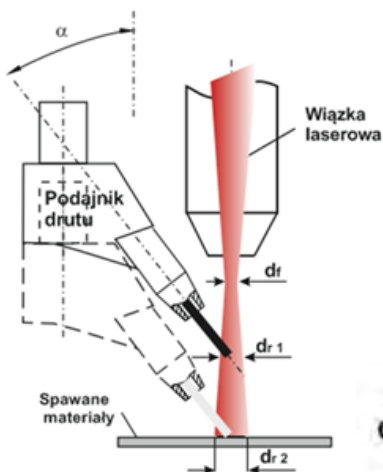
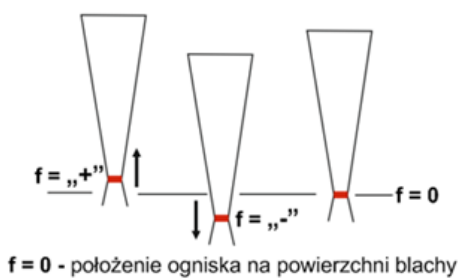
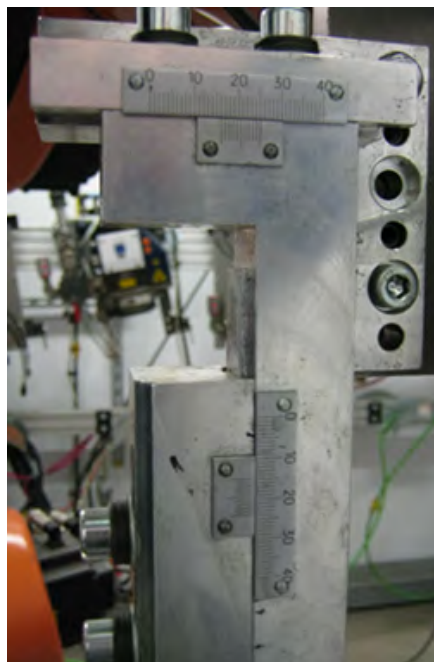


Fig. 5. Schematic diagram of the KUKA PCD 505 system (KUKA GmbH) for the monitoring of arc surfacing parameters and b) graphic recording of current and arc voltage waveforms



$$d_{og} = \frac{f_{og} \cdot d_{LLK}}{f_c}$$



(40H in accordance with PN) is toughening alloy steel having the pearlitic-ferritic structure. The content of carbon in the steel is restricted within the range of 0.3 % to 0.5%; alloying elements (chromium, silicon, manganese, nickel or molybdenum) do not exceed 5% [12–15]. Because of the high carbon equivalent ($CE = 0.77$), the above-named steel, characterised by limited weldability, can be found, among other things, in surfaced elements of actuators or hydraulic piston rods of mine supports used in excavation industry [16, 17].

The chemical composition and the mechanical properties of the test steel are presented in Table 1.

The filler metal used in the tests was filler metal wire grade OERLIKON INERTFIL

Fig. 6. a) schematic diagram of the determination of the position of the laser beam focus in relation to the surface of a material subjected to the surfacing process (parameter f), b) position of the electrode wire tip in relation to the plate surface and diameter of the laser beam focus, where d_{og} – laser beam focus diameter [mm], f_{og} – focal length of the focusing lens [mm], d_{LLK} – diameter of the optical fibre core [mm], f_c – focal length of the collimator lens [mm] and c) adjustment screws of the head used to change the position of the filler metal wire feeder

Table 1. Chemical composition and the mechanical properties of the base material used in the tests

Steel grade	Standard	Chemical composition, [%]									
	Analysis	C	Si	Mn	P	S	Cr	Cu	Ni	Mo	CE
41Cr4	PN-EN ISO 683-1	0.38 ÷ 0.45	max. 0.40	0.60 ÷ 0.90	max. 0.02	max. 0.03	0.90 ÷ 1.20	max. 0.55	max. 0.3	max. 0.1	0.77
	LBS/ZT/1/2019	0.39	0.26	0.66	0.01	0.001	1.04	0.18	0.16	0.04	0.73
Mechanical properties											
Steel grade	Standard	R _m [MPa]			R _e [MPa]			A ₅ [%]			
41Cr4	PN-EN ISO 683-1	1000 ÷ 1200			≥ 800			≥ 11			

307LSi (PN-EN ISO 14343-A: G/W 18 8 Mn). The above-named filler metal is used, among others, by companies surfacing hydraulic actuators made of steel 41Cr4. The chemical composition and the mechanical properties of the weld deposit are presented in Table 2.

The shielding gas used in the tests was the M12 mixture (Inoxline C2, PN-EN ISO 14175-M12 – ArC – 2.5), recommended by the manufacturer for surfacing with austenitic filler metal (Table 2).

Adjustment of the technological parameters of the hybrid surfacing process

The hybrid surfacing method requires the precise adjustment of a significantly larger number of process parameters than the conventional surfacing method. The designations and abbreviations presented below are related to technological parameters and conditions of the hybrid surfacing process: laser beam power – P [kW]; surfacing rate – V_n [m/min]; filler metal wire feeding rate – V_d [m/min]; surfacing current – I [A]; arc voltage – U [V]; arc voltage correction (arc source setting) – Kor. U [V]; distance between the laser beam focusing area and the electrode wire tip – a [mm]; position of the focus in relation to the surface of the plates subjected to surfacing – f [mm], electrode extension – D_w [mm] and heat input – Q [kJ/mm].

Heat input (Q) was identified in accordance with the PN-EN ISO 15614-14:2013-10 standard, sub-paragraph 8.12 [11], taking into consideration the total heat input supplied to the joint by

Table 2. Chemical composition and the mechanical properties of the filler metals used in the tests – in accordance with PN-EN ISO 14341:2011

Filler metal	Chemical composition, [%]				
	C	Si	Mn	Ni	Cr
LNM307	0.07	0.8	0.8	8.0	18.6
Mechanical properties					
Filler metal	Standard	R _m [MPa]	R _e [MPa]	A ₅ [%]	
LNM307	PN-EN ISO 14343-A	630	400	40	

electric arc and the laser beam in accordance with the following formula:

$$Q = \frac{(P + U \cdot I)}{V_n} 10^{-3}$$

where P – laser power [W], U – arc voltage [V], I – welding (surfacing) current [A], V_n – surfacing rate [mm/s].

The geometric measurements of the overlay weld were performed in accordance with the schematic diagram presented in Figure 7 [1].

The dilution of the base material in the overlay weld (W), signifying the proportion of the cross-sectional area of the partly molten base material F_w to the sum of the cross-sectional area of the excess weld metal of the overlay weld F_n and the base metal F_w, was calculated using the following formula [1]:

$$W = \frac{F_w}{F_n + F_w} \cdot 100\%$$

Similar to hybrid welding, laser + MAG hybrid surfacing can be performed in two

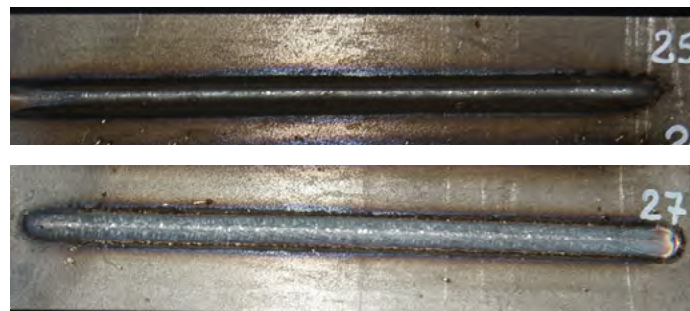
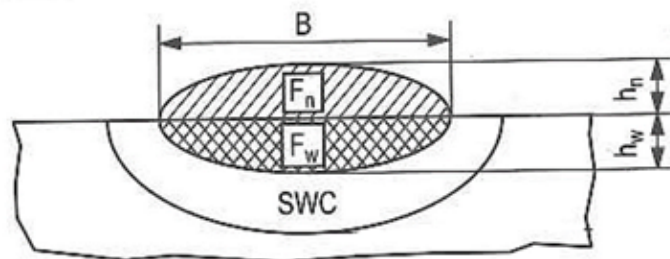


Fig. 9. Specimens obtained using the HLAW method-based surfacing process: a) specimen no 25 surfaced in the A-L (arc leading) configuration and b) specimen no. 27 surfaced in the L-A (laser leading) configuration

Fig. 7. Characteristics of the hybrid surfacing process, where B – overlay weld width, mm; F_n – area of the excess weld metal of the overlay weld, mm²; F_w – area of the partly molten base material, mm²; HAZ – head affected zone; h_n – excess weld metal height, mm; h_w – penetration depth, mm

configurations, i.e. in the A-L (arc leading) configuration, where the arc source is the leading surfacing power source in the process (Figure 8a) and in the L-A (laser leading) configuration, where the laser source is the leading surfacing power source in the process (Figure 8b).

The surfacing tests were performed in two configurations. The technological surfacing parameters used in the making of overlay welds on 5 mm thick plates are presented in Table 3. The overlay welds were characterised by the properly shaped uniform and smooth face along the entire length (Fig. 9). The recording of the current parameters performed using the PCD 505

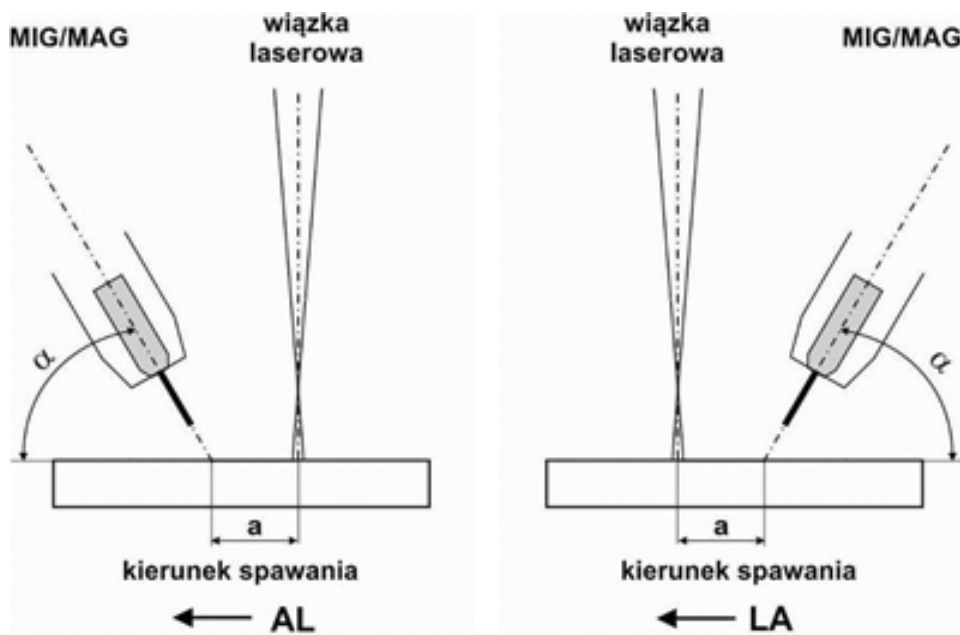


Fig. 8. Configurations of the hybrid laser surfacing process: a) A-L, i.e. arc leading configuration, b) L-A, i.e. laser leading configuration; α – MAG torch inclination angle, a – distance between the electrode wire tip and the laser beam

system revealed the stability of the surfacing process. The recorded hybrid surfacing process-related waveforms are presented in Figure 10.

Figure 11 presents the macrostructure and the results of geometric measurements related to the overlay welds. The macrostructural tests did not reveal the presence of internal welding imperfections.

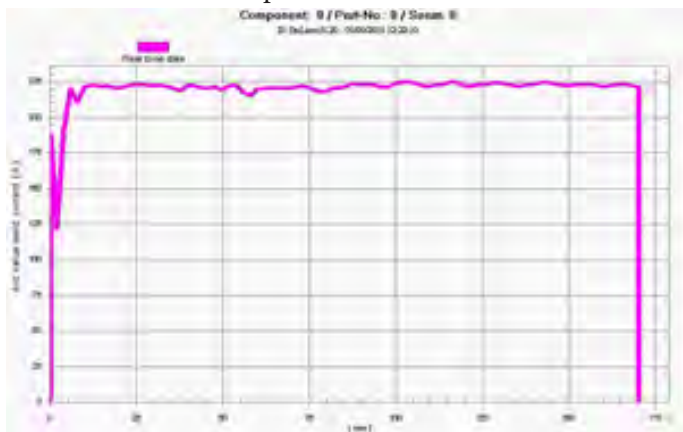
Table 4 presents the results of measurements concerning the area of the excess weld metal of the overlay weld, the degree of

Table 3. Hybrid surfacing process parameters

Specimen no.	P [kW]	Vn [m/min]	Vd [m/min]	I [A]	U [V]	Kor. U [V]	a [mm]	f [mm]	Dw [mm]	Q [kJ/mm]
25	1	1,2	8,5	225	26	3	2	+20	23	0,37
27	1	1,2	8,5	215	29	3	2	+20	23	0,36

25 – A-L: arc leading configuration;
26 – L-A: laser leading configuration

Specimen no. 25



Specimen no. 27

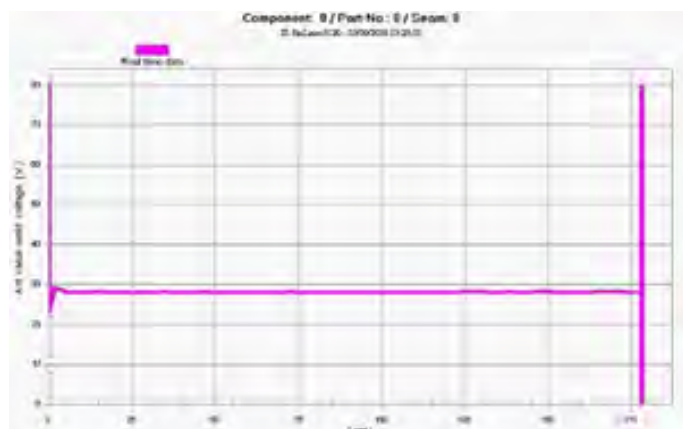
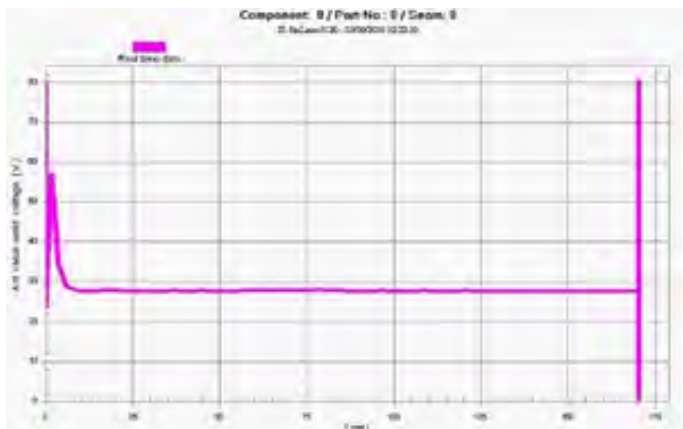
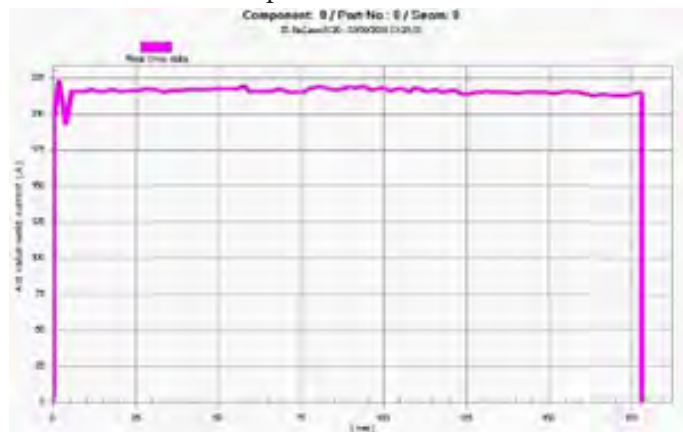


Fig. 10. Current-voltage parameters recorded by the PCD505 system in relation to the length of a section subjected to surfacing of specimen no. 25 and) specimen no. 27 (in accordance with Table 3)

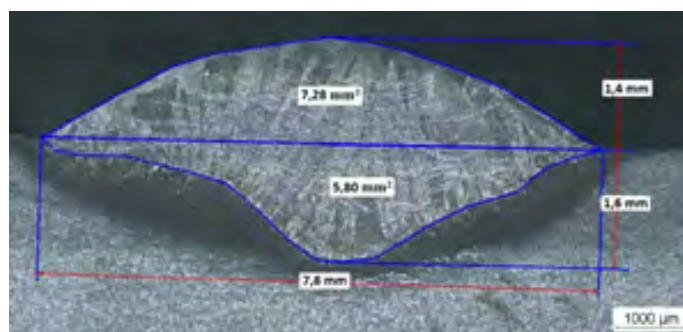
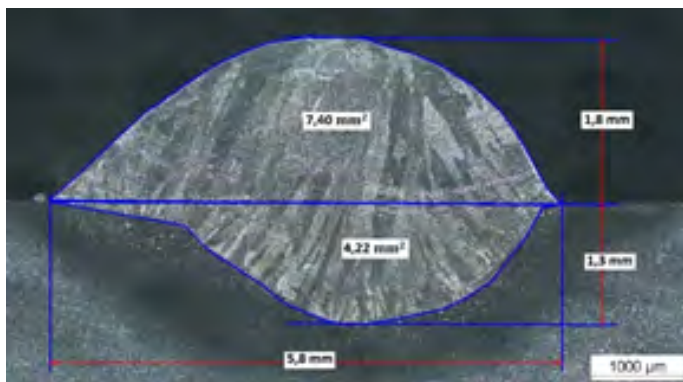


Fig. 11. Macrostructure and the geometric dimensions of the specimens made using the HLAW method: a) specimen 25 (L-A) and b) specimen 27 (A-L); in accordance with Table 3

Table 4. Area, geometric dimensions and the dilution of the base material in the overlay weld

Specimen no.	F_n mm ²	F_w mm ²	W %	h_n , mm	h_w , mm	B, mm
25 (A-L)	7.40	4.22	36	1.87	1.37	5.83
27 (L-A)	7.28	5.81	44	1.49	1.64	7.82

dilution of the base material in the overlay weld and the geometric dimensions of the overlay weld (in accordance with Fig 7). The planimetric measurements of the overlay welds revealed that the width of the overlay weld made in the laser leading configuration amounted to 7.8 mm

(Fig. 11). The overlay weld made in the L-A configuration was by 2 mm wider than the overlay weld made using the same parameters in the A-L configuration (Table 2).

The dilution of the base material in the overlay weld made in the A-L configuration

Table 5. Hybrid surfacing process parameters in relation to various levels of laser power

Specimen no.	P [kW]	V_n [m/min]	V_d [m/min]	I [A]	U [V]	Kor. U [V]	a [mm]	f [mm]	D_w [mm]	Q [kJ/mm]
37	0.5	1.2	8.5	215	29	3	2	+20	23	0.37
38	1			215	29					0.36
39	1.5			215	29					0.36

Surfacing in the L-A configuration

amounted to 36%. The dilution of the base material in the overlay weld made in the laser leading configuration amounted to 44% (Table 4). Because of the obtainment of the wider overlay weld, the remaining tests were performed in the L-A configuration.

The effect of the laser power on the shape of the overlay weld and the dilution of the base material in the overlay weld

One of the primary parameters of the hybrid surfacing process is the power of the laser, affecting the shape of the overlay weld and the dilution of the base material in the overlay weld. The research work involved the performance



Fig. 12. Face of the specimens made using the HLAW method; in accordance with Table 5

of surfacing tests in relation to three levels of laser power. The surfacing parameters are presented in Table 5. The specimens after the surfacing process are presented in Figure 19.

Visual tests revealed that the overlay welds were characterised by the spatter-free uniform

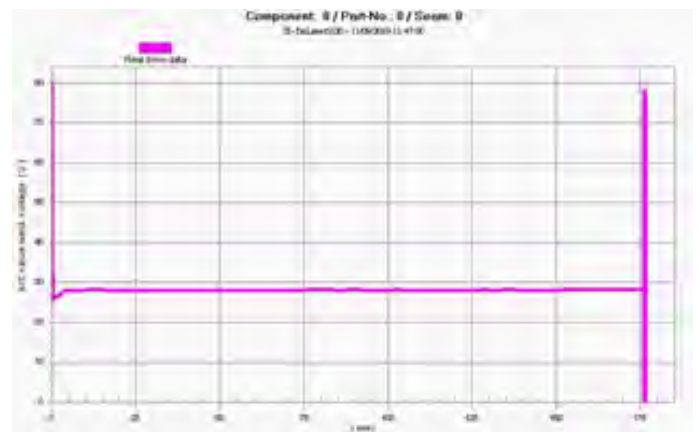
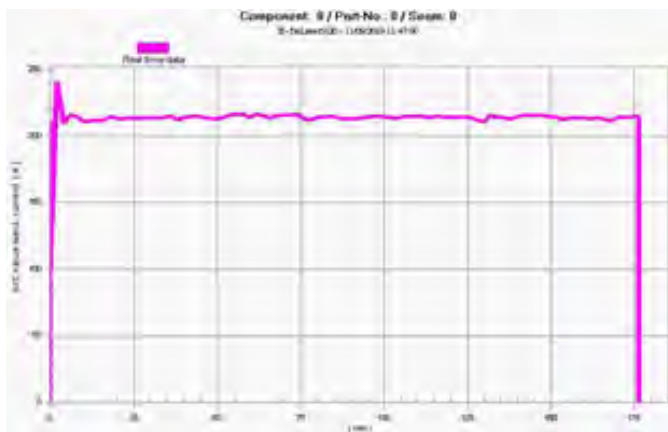


Fig. 13. Current-voltage parameters of the surfacing process recorded by the PCD505 system in relation to the length of a section subjected to surfacing, made using a laser power of 1 kW (specimen no. 38): a – welding (surfacing) current and b – arc voltage

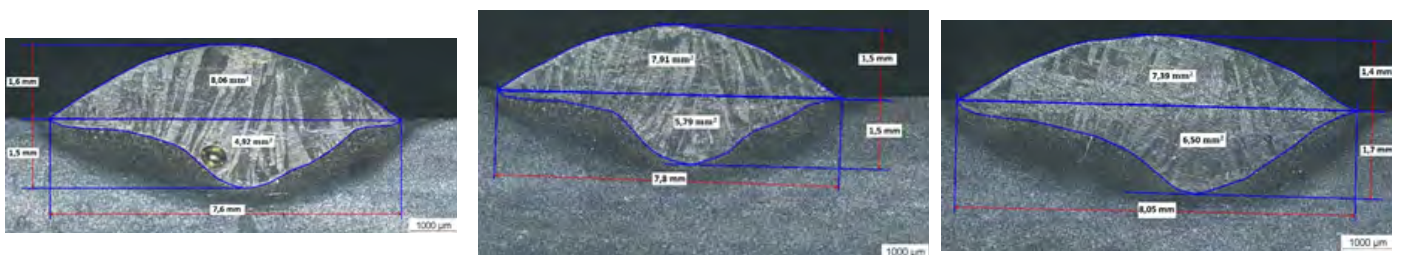


Fig. 14. Macrostructure and the geometric dimensions of the specimens made using the HLAW method: a) specimen 37, b) specimen 38, c) specimen 39; in accordance with Table 5

Table 6. Area, geometric dimensions and the dilution of the base material in the overlay weld

Specimen no.	F_n mm ²	F_w mm ²	W %	h_n , mm	h_w , mm	B, mm
37	8.06	4.92	37	1.62	1.51	7.66
38	7.92	5.22	39	1.59	1.58	7.86
39	7.40	6.51	46	1.41	1.77	8.06

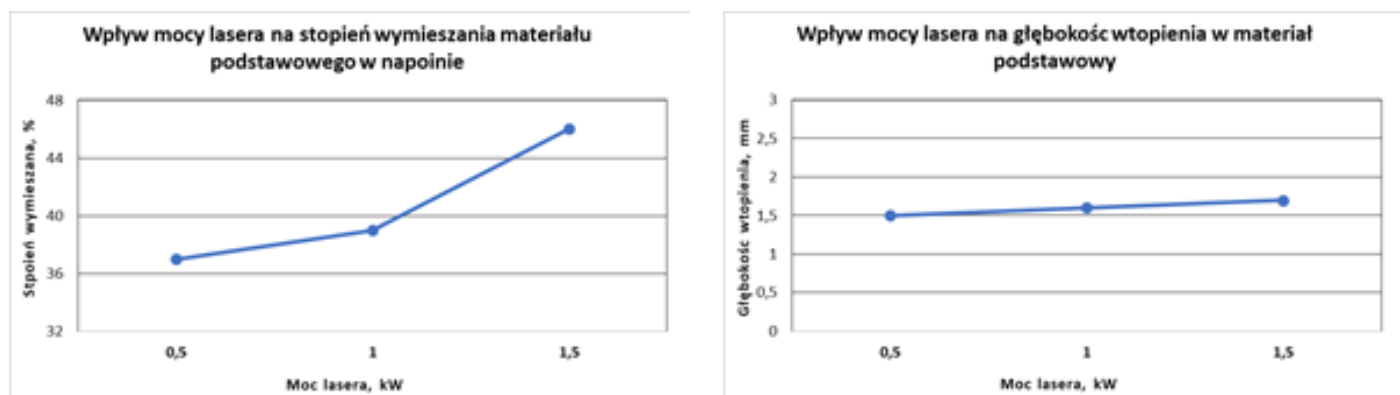


Fig. 15. Effect of laser power in the HLAW process on: a) dilution of the base material in the overlay weld and b) depth of penetration into the base material; in accordance with Table 6

and smooth face and by the lack of surface welding imperfections (Fig. 12).

The recording of the process parameters performed using the PCD 505 system did not reveal the disturbance of the process stability or important changes within the waveforms of MAG welding current and arc voltage (Fig. 13).

Figure 14 presents the macrostructure and the results of geometric measurements related to the overlay welds (Table 5)

The macroscopic tests revealed the presence of welding imperfection no. 200, i.e. gas pore (in accordance with PN-EN ISO 6520-1)

in specimen no. 37 made using a laser power of 0.5 kW (Fig. 14a). The remaining specimen did not contain internal welding imperfections in the overlay weld area or in the HAZ (Fig. 14b, c). Planimetric measurements revealed that the specimens were characterised by a similar width of approximately 8 mm (Table 6).

In the overlay weld made using a laser power of 0.5 kW, the dilution of the base material in the overlay weld amounted to 37%. An increase in laser power to 1.5 kW resulted in an increase in dilution by 9%, i.e. to 46% (Fig. 15a). In relation to surfacing performed using a laser

Table 7. Hybrid surfacing process parameters

Specimen no.	P [kW]	V_n [m/min]	V_d [m/min]	I [A]	U [V]	Kor. U [V]	a [mm]	f [mm]	D_w [mm]	Q [kJ/mm]
40	0.5	0.6	8.5	215	29	3	2	+20	23	0.67
41			10	225	30					0.72
42			12	250	31					0.82
28	0.5	1.2	8.5	215	29	3	2	+20	23	0.33
29			10	220	30					0.35
30			12	270	31					0.44
43	0.5	1.6	8.5	220	29	3	2	+20	23	0.25
44			10	245	30					0.29
45			12	270	31					0.33

Surfacing in the L-A configuration

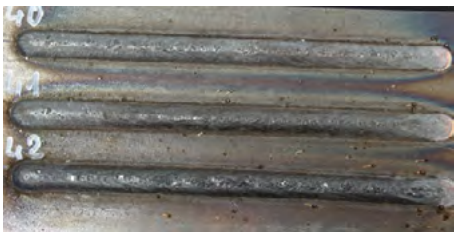


Fig. 16. Face of the specimens made using the HLAW method and surfacing rate of 0.6 m/min; in accordance with Table 7

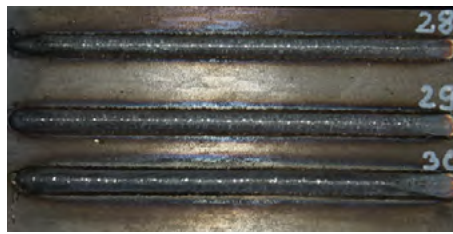


Fig. 17. Face of the specimens made using the HLAW method and surfacing rate of 1.2 m/min; in accordance with Table 7



Fig. 18. Face of the specimens made using the HLAW method and surfacing rate of 1.6 m/min; in accordance with Table 7

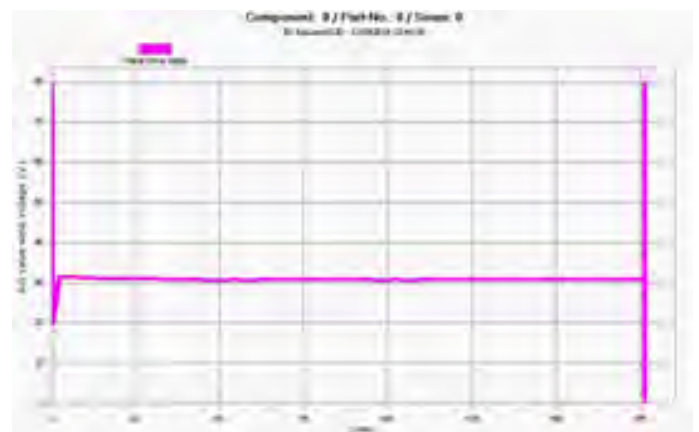
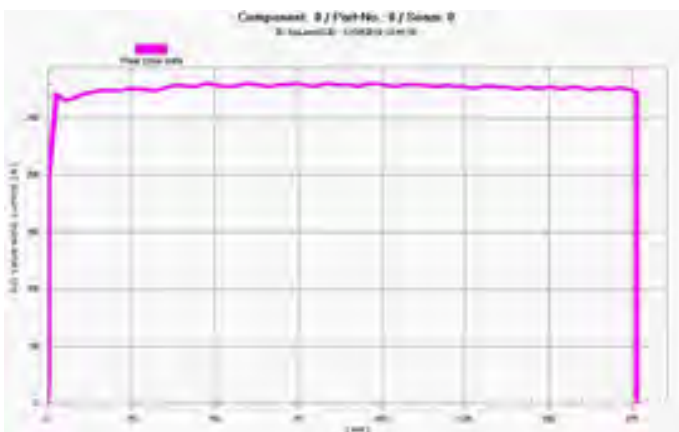
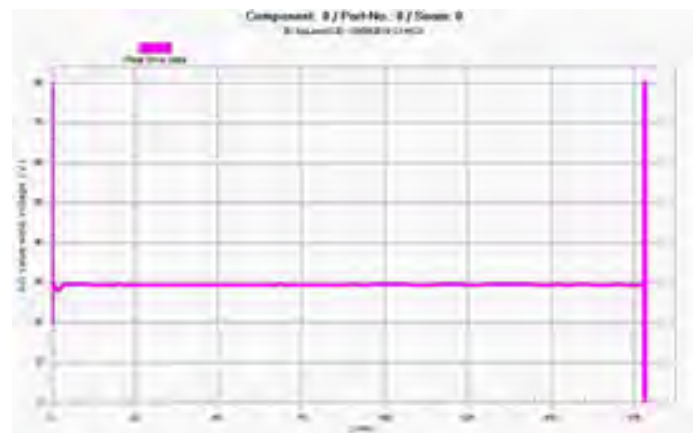
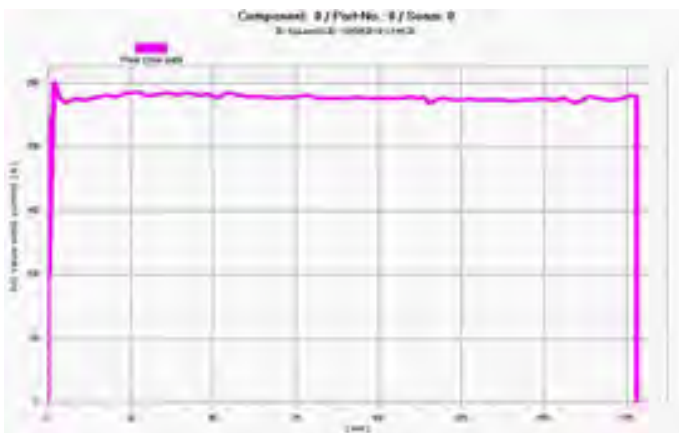
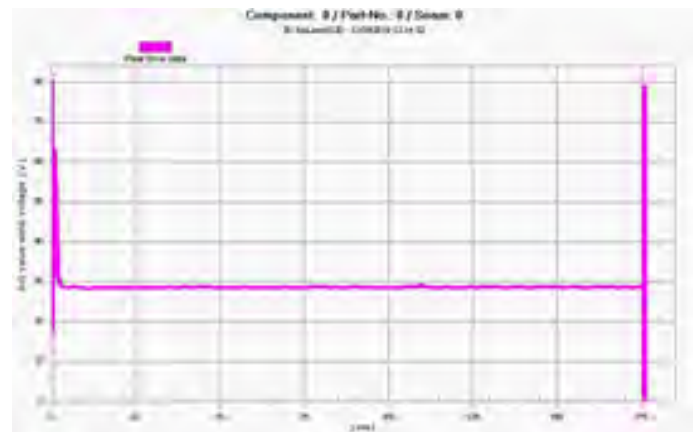
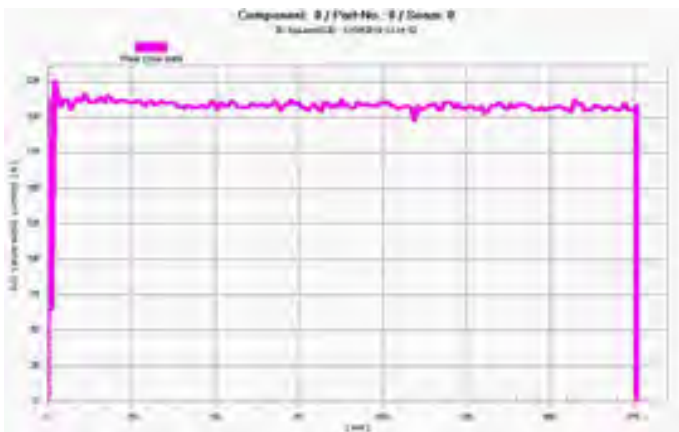


Fig. 19. Selected current-voltage parameters recorded by the PCD505 system in relation to the length of a section subjected to surfacing: a) specimen no. 40, b) specimen no. 29 and c) specimen no. 45 (in accordance with Table 7)

power of 0.5, the measured depth of penetration into the base material amounted to 1.5 mm. An increase in laser power to 1.5 kW resulted in an increase in penetration depth to 1.7 mm (Fig. 15b).

The effect of the surfacing rate on the shape of the overlay weld and the dilution of the base material in the overlay weld

The research work involved the performance of hybrid surfacing aimed to determine the effect of a surfacing rate on the shape and geometry of overlay welds. The surfacing tests were performed applying 3 surfacing rates and filler metal wire feeding rates (Table 7).

The specimens obtained after the surfacing process are presented in Figures 16, 17 and 18. Visual tests revealed that the specimens made using a surfacing rate of 0.6 m/min (Fig. 16) contained welding imperfection no. 600, i.e. spatter (in accordance with PN-EN ISO 6520-1) [19]. The remaining specimens (overlay welds) were characterised by the uniform and smooth face and were free from spatter

(Fig. 24, 25).

The observation and recording of the process parameters performed using the PCD 505 system revealed the stability of the process within the waveforms of MAG welding current and arc voltage as well as in relation to surfacing rates and filler metal wire feeding rates (Fig. 19).

Figure 20 presents the macrostructure and the results of geometric measurements related to the overlay welds. The macrostructural tests did not reveal the presence of internal welding imperfections in the overlay weld.

Table 8 presents measurement results concerning the area of the excess weld metal of the overlay weld, the degree of dilution of the base material in the overlay weld and the geometric dimensions of the overlay welds.

The widest overlay weld width amounting to 12 mm was obtained in relation to a surfacing rate of 0.6 m/min and a filler metal wire feeding rate of 12 m/min. An increase in the surfacing rate to 1.6 m/min reduced the overlay weld width to less than 8 mm (Fig. 21a). In relation to a surfacing rate of 0.6 m/min, the overlay weld height amounted to 6.7 mm. An increase

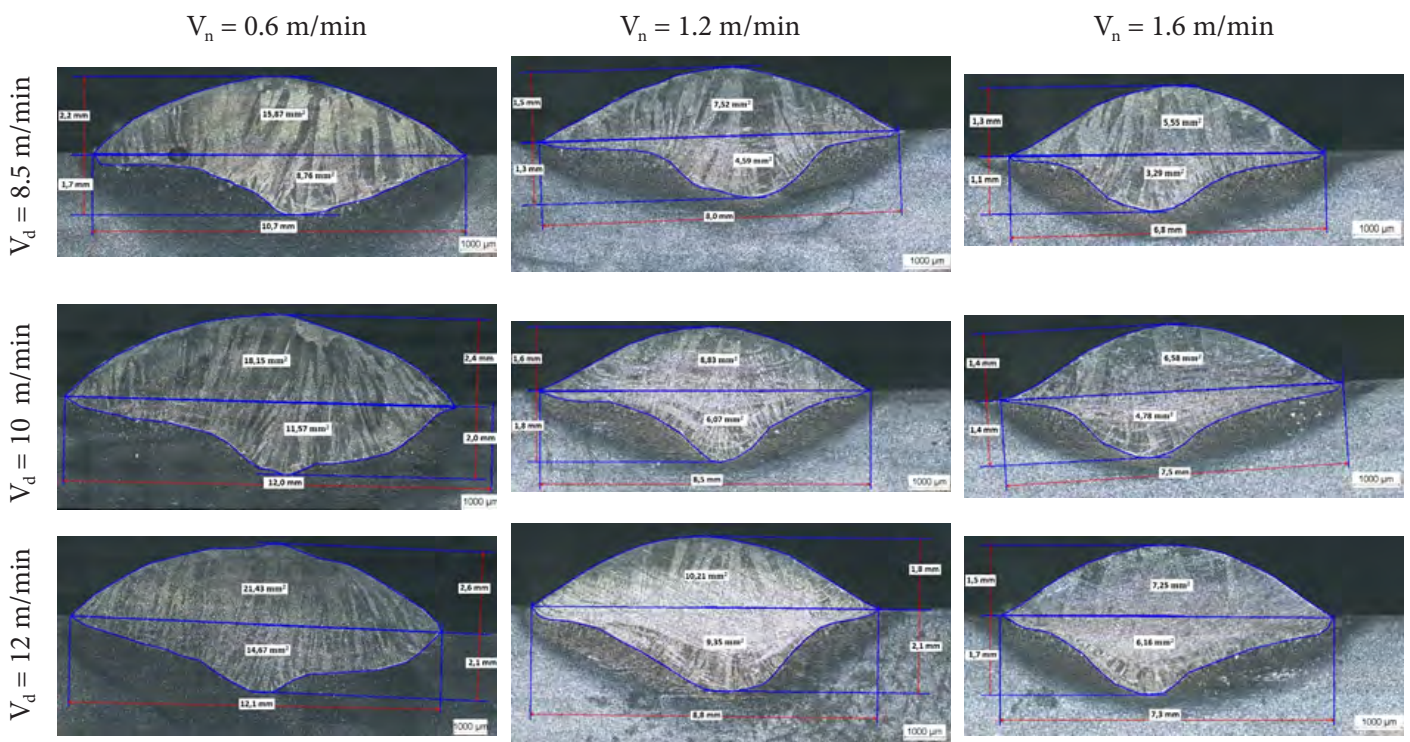


Fig. 20. Macrostructure and the geometric dimensions of the specimens made using the HLAW method and various surfacing rates in relation to filler metal wire feeding rates, in accordance with Table 7

Table 8. Area, geometric dimensions and the dilution (of the base material in the overlay weld)

Specimen no.	F_n mm ²	F_w mm ²	W %	h_n , mm	h_w , mm	B, mm
40	15.87	8.76	35	2.24	1.72	10.74
41	18.16	11.58	38	2.46	2.03	12.10
42	21.44	14.67	40	2.67	2.17	12.13
28	7.52	4.59	37	1.55	1.38	8.04
29	8.84	6.08	40	1.66	1.84	8.58
30	10.22	9.35	47	1.81	2.13	8.84
43	5.56	3.30	37	1.33	1.12	6.87
44	6.59	4.79	42	1.49	1.43	7.58
45	7.26	6.17	45	1.55	1.74	7.31

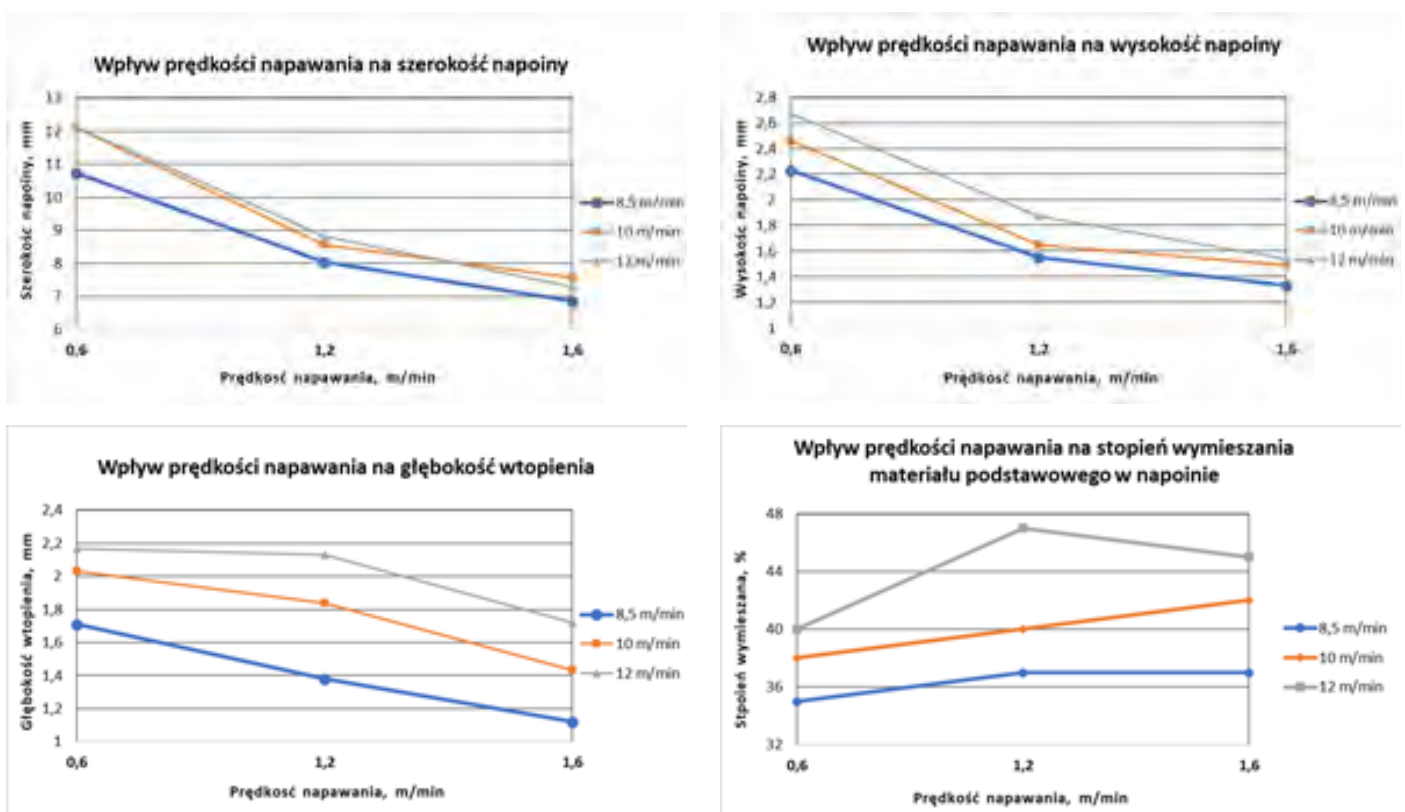


Fig. 21. Effect of the HLAW surfacing rate in relation to the filler metal wire feeding rate on: a) overlay weld width, b) overlay weld height, c) penetration depth and d) dilution of the base material in the overlay weld; in accordance with Table 8

in the surfacing rate reduced the overlay weld height to 1.5 mm (Fig. 21b).

A penetration depth of 2.1 mm was obtained in relation to a surfacing rate of 0.6 m/min (Fig. 21c). The lowest dilution of the base material in the overlay weld was obtained in relation to a surfacing rate of 0.6 m/min and a filler metal wire feeding rate of 8.5 m/min. The highest degree of dilution was obtained in relation to a surfacing rate of 1.2 m/min and a filler metal wire feeding rate of 12 m/min (Fig. 21d).

The effect of the distance between the laser and the electrode tip on the shape of the overlay weld and the dilution of the base material in the overlay weld

In accordance with the PN-EN ISO 15609 standard, the hybrid process is the one where the use of two welding power sources leads to the formation of one common weld pool. In addition, in accordance with the above-named standard, a process where an excessively long distance

between two welding power sources leads to the formation of two separate weld pools is referred to as the combined process.

The research involved the performance of surfacing tests aimed to determine the value of parameter *a*, defining the distance between the laser and the electrode tip. The surfacing tests were performed in relation to distance *a* = 2 mm, 6 mm and 10 mm as well as various surfacing rates and filler metal wire feeding rates. The surfacing process parameters in relation to various values of the distance between the laser and the electrode tip are presented in Table 9. The obtained overlay welds are presented in Figures 22–24. The overlay welds were characterised by the uniform spatter-free face and the lack of surface welding imperfections.

The recording of parameters obtained using a PCD 505 system did not reveal any disturbance of the process stability or significant changes in the waveforms of MAG welding current and arc voltage as well as changes in

surfacing rates and filler metal wire feeding rates (Fig. 25).

Figure 26 presents the macrostructure and the results of geometric measurements of the overlay welds. Table 10 presents measurement results concerning the area of the excess weld metal of the overlay weld, the degree of dilution (of the base material in the overlay weld) and geometric dimensions (in accordance with Fig. 7).

Planimetric tests revealed that in relation to *a* = 6 mm and *V_d* = 12 m/min, the overlay weld width amounted to 9.37 mm (specimen no. 33, Table 10). The narrowest overlay weld width, amounting to 8 mm, was obtained in relation to *a* = 2 mm and *V_d* = 8.5 m/min (Fig. 26a).

The lowest degree of the dilution of the base material in the overlay weld amounted to 37% and was obtained in relation to *a* = 2 mm and *V_d* = 8.5 m/min as well as in relation to *a* = 6 mm and *V_d* = 8.5 m/min. The highest degree of the dilution amounting to 47% was obtained

Table 9. Parameters of the hybrid surfacing process in relation to various values of the distance between the laser and the electrode tip

Specimen no.	P [kW]	V _n [m/min]	V _d [m/min]	I [A]	U [V]	Kor. U [V]	a [mm]	f [mm]	D _w [mm]	Q [kJ/mm]
28	0.5	1.2	8.5	215	29	3	2	+20	23	0.33
29			10	220	30					0.35
30			12	270	31					0.44
31	0.5	1.2	8.5	215	29	3	6	+20	23	0.33
32			10	245	30					0.39
33			12	270	31					0.44
34	0.5	1.2	8.5	220	29	3	10	+20	23	0.34
35			10	245	30					0.39
36			12	270	31					0.44

Surfacing in the L-A configuration



Fig. 22. Face of the specimens made using the HLA method and distance *a* = 2 mm; in accordance with Table 9



Fig. 23. Face of the specimens made using the HLA method and distance *a* = 6 mm; in accordance with Table 9

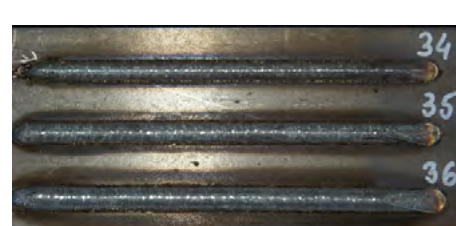


Fig. 24. Face of the specimens made using the HLA method and distance *a* = 10 mm, in accordance with Table 9

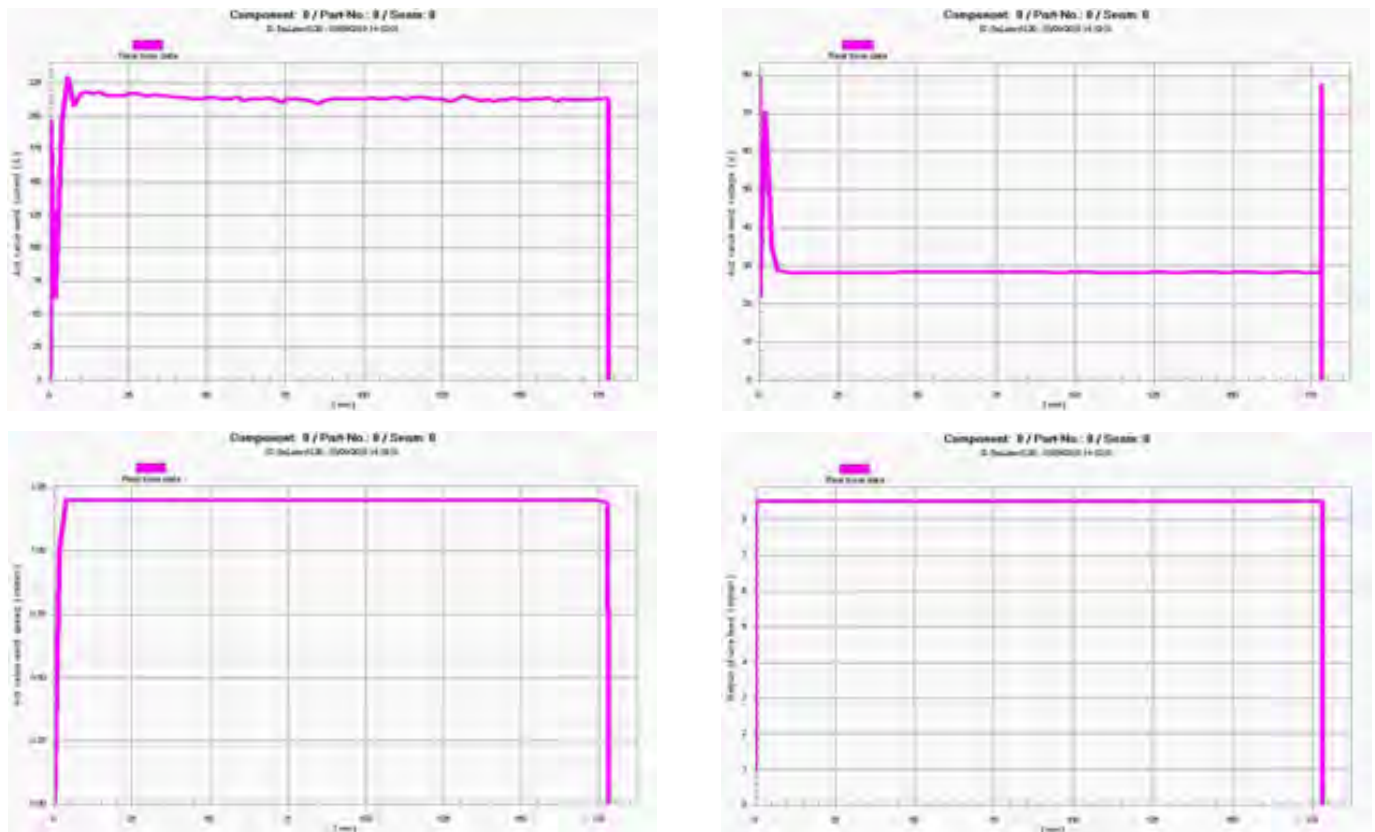


Fig. 25. Primary parameters of the hybrid surfacing of specimen no. 31, in accordance with Table 9, in relation to the length of a section subjected to surfacing: a – surfacing current, b – arc voltage, c – surfacing rate and d – filler metal wire feeding rate

Table 10. Area, geometric dimensions and the dilution (of the base material in the overlay weld)

Specimen no.	F_n mm ²	F_w mm ²	W %	h_n , mm	h_w , mm	B, mm
28	7.52	4.59	37	1.55	1.38	8.04
29	8.84	6.08	40	1.66	1.84	8.58
30	10.22	9.35	47	1.81	2.13	8.84
31	7.69	4.20	35	1.56	1.33	8.10
32	9.23	6.06	39	1.76	1.82	8.62
33	10.56	8.77	45	1.85	2.20	9.37
34	7.75	4.61	37	1.62	1.44	8.29
35	9.14	6.59	41	1.76	1.84	8.55
36	10.09	8.36	45	1.82	2.15	9.15

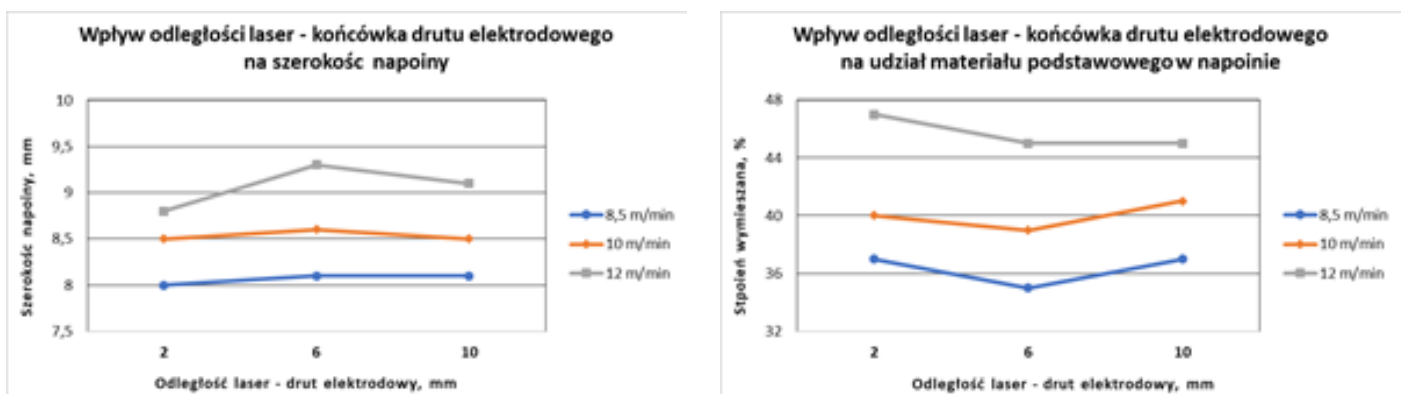


Fig. 26. Effect of parameter a in the HLAW process on: a) overlay weld width, b) dilution of the base material in the overlay weld, in accordance with Table 9

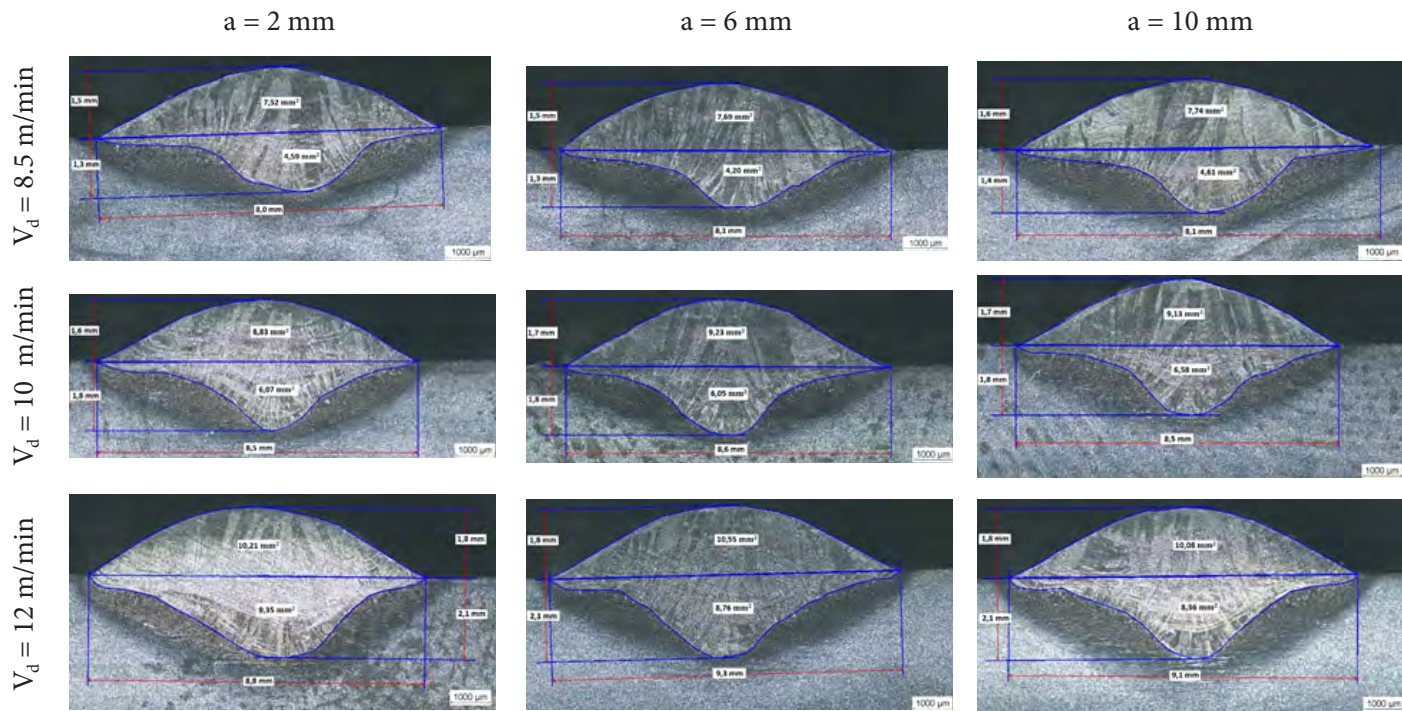


Fig. 27. Macrostructure and the geometric dimensions of the specimens made using the HLAW method and various surfacing rates in relation to filler metal wire feeding rates, in accordance with Table 9

in relation to $a = 2 \text{ mm}$ and $V_d = 12 \text{ m/min}$ (Fig. 26b).

The specimen made using distance $a = 2 \text{ mm}$, $P=0.5 \text{ kW}$, $V_d = 8.5 \text{ m/min}$ and $V_n = 1.2 \text{ m/min}$ (no. 28) was subjected to microstructural tests. The tests involved the base material, the HAZ and the overlay weld. The central area of the overlay weld contained the austenitic structure (251 HV₁₀), the HAZ contained the martensitic structure (594 HV₁₀), whereas the base material contained the pearlitic-ferritic structure (191 HV₁₀) (Fig. 28).

Guidelines concerning steel 41Cr4 specify that, before surfacing, the steel should be heated

up to a temperature below the temperature of the end of the martensitic transformation M_f . After surfacing the steel should be cooled below M_f (hardened). Finally, the steel should be subjected to high-temperature tempering (500–670°C) – heating below temperature A_1 [14]. The hybrid surfacing tests involved preheating. The minimum preheating temperature T_p in °C for a 5 mm thick plate made of steel 41Cr4 was calculated using the Seferian formula [14]:

$$T_p = 350\sqrt{(CET[1 + 0,005g] - 0,25)} \text{ [}^\circ\text{C]}$$

where T_p – preheating temperature, °C; g – plate thickness, mm; CET – carbon equivalent.

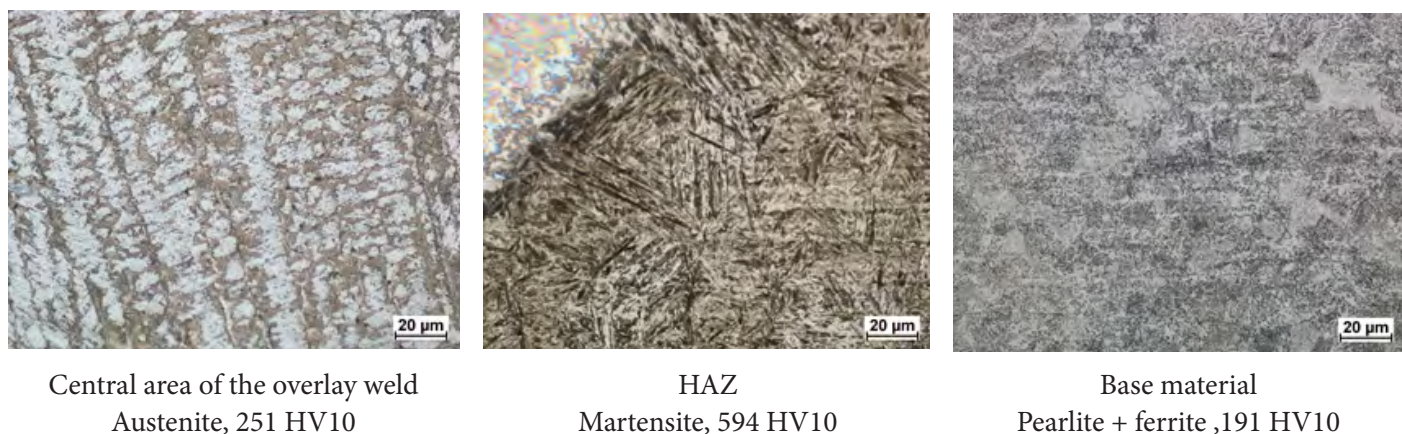


Fig. 28. Microstructure of the overlay weld – specimen no. 28; in accordance with Table 10

It was assumed that the preheating temperature amounted to 250°C. The remaining process parameters were identical to those used in relation to specimen no. 30 (Table 9).

The selected overlay welds were subjected to hardness tests performed in accordance with the schematic diagram presented in Figure 29. The results of the measurements of hardness distribution in the specimens subjected and not subjected to preheating are presented in Figure 30.

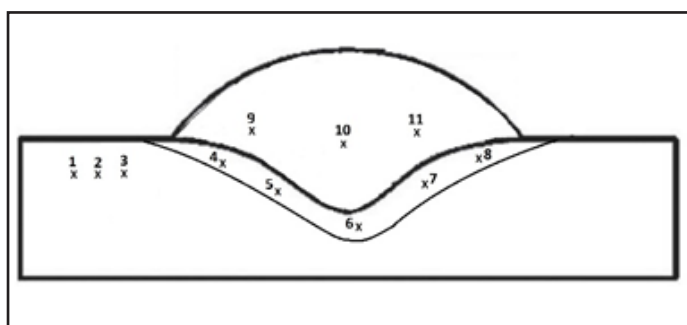


Fig. 29. Distribution of hardness in the cross-section of the overlay weld

In the surfaced specimen not subjected to preheating the highest value of hardness, amounting to 645 HV₁₀, was measured in the HAZ (point 7). The application of preheating up to a temperature of 250°C reduced the hardness in the HAZ to 515 HV₁₀ (point 7). The lowest hardness was measured in the base material area and amounted to 195 HV₁₀. The average value of hardness in the overlay weld axis made with and without preheating amounted to 249 HV₁₀.

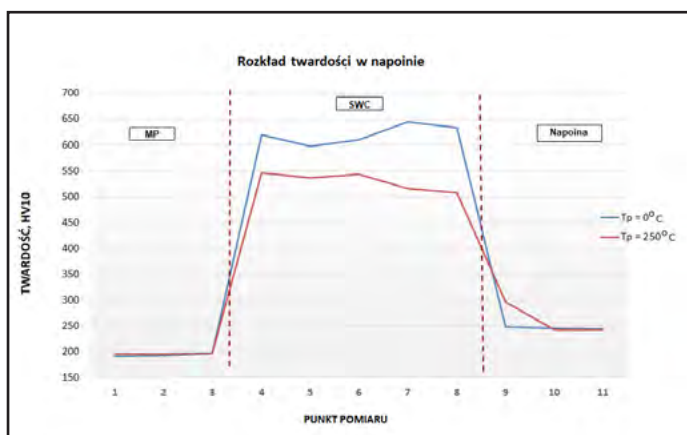


Fig. 30. Distribution of hardness HV10 in the cross-section of the overlay weld subjected and not subjected to preheating

Summary

The process of hybrid surfacing is characterised by many variables affecting the final result of the surfacing process. The hybrid method requires the precise adjustment, correlation and the optimisation of more process parameters than in the laser powder surfacing or flux-cored arc surfacing process. It is necessary to adjust the current parameters of welding arc and those of the laser beam (size and location of the focus, focusing system, laser beam power etc.). It is also necessary to precisely position both welding power sources in relation to each other (distance between the laser and the electrode tip).

The tests revealed that the overlay welds made in the laser leading (L-A) configuration were characterised by the wider overlay weld face than those made using the arc leading configuration (A-L).

The stable hybrid surfacing process requires the defocused beam (lifting the beam upwards by a minimum of 20 mm), a laser beam power of 0.5 kW, the distance between the laser and the electrode tip amounting to 6 mm (parameter a), a surfacing rate of 1.2 m/min and a filler metal wire feeding rate of 8.5 m/min. The above-named configuration of the system combined with appropriately adjusted parameters enables the obtainment of proper overlay welds having the appropriately wide face and the lowest degree of dilution.

Steel 41Cr4 has the pearlitic-ferritic structure. The microstructural test of the overlay weld revealed the presence of the austenitic structure in the central area (251 HV₁₀) and the martensitic structure in the HAZ (594 HV₁₀). The HAZ was characterised by an increase in hardness up to 645 HV₁₀. The preheating process led to the reduction of hardness by 95 HV₁₀.

The obtainment of a hardness of 380 HV₁₀ (satisfying the welding procedure qualification-related requirements of standard PN-EN ISO 15614-7) requires the performance of post-weld heat treatment (hardening and high-temperature tempering).

References

- [1] Pilarczyk J (red.): Poradnik Inżyniera. Spawalnictwo, tom 2. Wydawnictwa Naukowo-Techniczne, Warszawa 2005, 2014.
- [2] Klimpel A.: Napawanie i natryskiwanie cieplne. Wydawnictwa Naukowo Techniczne, Warszawa, 2000.
- [3] Brian M. Victor: Hybrid laser arc welding. Edison Welding Institute, ASM Handbook, Volume 6A, Welding Fundamentals and Processes, 2011.
- [4] Banasik M., Turyk E., Urbańczyk M.: Spawanie hybrydowe laser + MAG elementów urządzeń dźwigowych wykonanych ze stali ulepszonej cieplnie S960QL. Przegląd Spawalnictwa, 2017, vol. 89, no. 5, pp. 23–27.
- [5] Urbańczyk M., Banasik M., Stano S., Adamiec J.: Wpływ technologii spawania hybrydowego na strukturę i właściwości stali o podwyższonej granicy plastyczności S960QL. Biuletyn Instytutu Spawalnictwa, 2018, no. 5.
- [6] Urbańczyk M.: Wpływ technologii spawania hybrydowego (laser + MAG) na strukturę i właściwości stali o wysokiej granicy plastyczności S960QL. Doctor's dissertation, Katowice, 2018.
- [7] Hybrid welding. TRUMPF. <http://www.trumpf-laser.com/en/solutions/applications/laser-welding/hybrid-welding.html>.
- [8] Banasik M., Urbańczyk M.: Spawanie metodą hybrydową laser + MAG różnych rodzajów złączy. Biuletyn Instytutu Spawalnictwa, 2017, no. 1.
- [9] PN-EN ISO 15609-6:2013 Specyfikacja i kwalifikowanie technologii spawania metali. Instrukcja technologiczna spawania. Część 6: Spawanie hybrydowe laserowo-łukowe.
- [10] Patent no. US 2017/0165794 A1 published on 15.06.2017. "Hybrid laser cladding composition and component therefrom". Applicant: Caterpillar Inc. Peoria, IL (US).
- [11] Norma PN-EN ISO 15614-14:2013, Specyfikacja i kwalifikowanie technologii spawania metali. Badanie technologii spawania. Część 14 Spawanie hybrydowe laserowo-łukowe stali, niklu i stopów niklu
- [12] Tasak E.: Metalurgia spawania. JAK, Kraków, 2008.
- [13] AKROSTAL <https://akrostal.pl/stale/40h-41cr41-7035/>
- [14] Wojno T., Kędzia J., Mirski Z., Reiner J.: Hybrydowe spawanie stali 41Cr4 z wykorzystaniem promieniowania laserowego i nagrzewania indukcyjnego. Przegląd Spawalnictwa, 2013, vol. 85, no. 7.
- [15] PN-EN ISO 683-1, Stale do obróbki cieplnej, stale stopowe i stale automatowe. Część 1. Stale niestopowe do hartowania i odpuszczania.
- [16] WPQR no. IS/ZT/175/06, developed by Instytut Spawalnictwa 2006.
- [17] WPQR no. IS/ZT/1194/16, developed by Instytut Spawalnictwa 2016
- [18] Urbańczyk M.: Napawanie hybrydowe laser + MAG. Rozpoznanie i ocena możliwość metody przy wykorzystaniu uniwersalnej głowicy hybrydowej i lasera dyskowego. Research work no. Ac-154 (ST 394), Łukasiewicz–Instytut Spawalnictwa, 2019
- [19] PN-EN ISO 6520-1 Spawanie i procesy pokrewne. Klasyfikacja geometrycznych niezgodności spawalniczych w metalach. Część 1: Spawanie.